FIELDS OF VALUES AND INCLUSION REGIONS FOR MATRIX PENCILS *

MICHIEL E. HOCHSTENBACH[†]

This paper is dedicated with pleasure to Prof. Varga.

Abstract. We are interested in (approximate) eigenvalue inclusion regions for matrix pencils (A, B), in particular of large dimension, based on certain fields of values. We show how the usual field of values may be efficiently approximated for large Hermitian positive definite B, but also point out limitations of this set. We introduce four field of values based inclusion regions, which may effectively be approximated, also for large pencils. Furthermore, we show that these four sets are special members of two families of inclusion regions, of which we study several properties. Connections with the usual harmonic Rayleigh–Ritz method and a new variant are shown, and we propose an automated algorithm which gives an approximated inclusion region. The results are illustrated by several numerical examples.

Key words. inclusion region, exclusion region, matrix pencil, numerical range, field of values, generalized eigenvalue problem, large sparse matrix, harmonic Rayleigh–Ritz, harmonic Ritz values, Krylov space

AMS subject classifications. 65F15, 65F50, 65F30, 65F35, 47A12

1. Introduction. For $n \times n$ matrices A and B, consider the generalized eigenvalue problem

$$(1.1) \qquad A\mathbf{x} = \lambda B\mathbf{x}.$$

We are interested in practical (approximate) spectral inclusion regions for (1.1), in particular for large pencils, based on certain fields of values. The field of values of an $n \times n$ real or complex matrix A,

$$W(A) = \{\mathbf{x}^*A\mathbf{x} : \|\mathbf{x}\| = 1\},$$

where $\| \cdot \|$ denotes the two-norm, has been extensively studied; see, for instance, [2].

The field of values (or numerical range) of a matrix pencil (A, B) was defined as

$$(1.2) \qquad W(A, B) = \{\lambda \in \mathbb{C} : \mathbf{x}^*(A - \lambda B)\,\mathbf{x} = 0, \quad \mathbf{x} \in \mathbb{C}^n, \quad \|\mathbf{x}\| = 1\},$$

and examined in [4, 7]; see also [5].

If B is singular, then the pencil (A, B) may have an infinite eigenvalue. However, by definition the set (1.2) does not contain the point at infinity. As a consequence, from this definition, $W(A, B)$ is not necessarily a spectral inclusion region. Therefore, we will work with a slightly modified definition and add the point at infinity to $W(A, B)$ if B is singular. A homogeneous expression equivalent to this is the set

$$W(A, B) = \left\{\frac{\alpha}{\beta} : \mathbf{x}^*(\beta A - \alpha B)\,\mathbf{x} = 0, \quad \|\mathbf{x}\| = 1, \quad (\alpha, \beta) \neq (0, 0)\right\}.$$

We can also use yet another equivalent definition: if there exists a nonzero $\mathbf{x}$ for which $\mathbf{x}^*A\mathbf{x} = \mathbf{x}^*B\mathbf{x} = 0$, then $W(A, B) = \mathbb{C} \cup \{\infty\}$; otherwise

$$W(A, B) = \left\{\frac{\mathbf{x}^*A\mathbf{x}}{\mathbf{x}^*B\mathbf{x}} : \mathbf{x} \neq \mathbf{0}\right\},$$

where $1/0$ is understood as the point at infinity. Note that all definitions can be formulated to range over all nonzero vectors or over all vectors of unit norm with straightforward adaptations.

If B is Hermitian positive definite (HPD), it can be decomposed as $B = LL^*$ (for instance, the matrix square root or the Cholesky factorization), and we have (cf. [7])

$$W(A, B) = \left\{ \frac{\mathbf{x}^* A \mathbf{x}}{\mathbf{x}^* B \mathbf{x}} : \mathbf{x} \neq \mathbf{0} \right\} = \left\{ \frac{\mathbf{y}^* L^{-1} A L^{-*} \mathbf{y}}{\mathbf{y}^* \mathbf{y}} : \mathbf{y} \neq \mathbf{0} \right\} = W(L^{-1} A L^{-*}).$$

One of the properties of $W(A, B)$ is that it is unbounded if (and only if) $0 \in W(B)$ [4]. Since our interest is in spectral inclusion regions for the pencil (A, B), this is clearly an unattractive feature: if B is nonsingular but $0 \in W(B)$, then the spectrum is bounded, but the inclusion region $W(A, B)$ is unbounded, and therefore not very informative. This motivates us to examine other field of values types of inclusion regions.

The rest of the paper has been organized as follows. In Section 2, we introduce four inclusion regions of field of values type for matrix pencils. Section 3 studies the question how to efficiently approximate $W(A, B)$ for HPD B, for matrices of both small and large dimension. Section 4 examines how to obtain eigenvalue inclusion regions based on fields of values for non HPD B; we will exploit the sets introduced in Section 2. Section 5 extends these four special inclusion regions to two different families of inclusion regions. By varying a parameter (the *target*), we can generate infinitely many inclusion regions. We will study several theoretical properties of the sets, as well as their practical computation.

Section 6 points out connections of these families with the usual harmonic Rayleigh–Ritz method for the generalized eigenvalue problem, and a new variant of this approach (the *left-harmonic Rayleigh–Ritz* method). Sections 7 gives an automated algorithm and an additional numerical experiment. We end with some conclusions in Section 8.

2. Four inclusion regions of field of values type for matrix pencils. If B is nonsingular, then the spectrum of $B^{-1}A$ coincides with that of the pencil (A, B). As a consequence,

$$(2.1) \qquad\qquad W(B^{-1}A)$$

is a spectral inclusion region for (1.1). Similarly,

$$(2.2) \qquad\qquad W(AB^{-1})$$

is also an inclusion region for (1.1); note that both sets are generally not equal to $W(A, B)$.

Next, we consider two different inclusion regions, which, to our best knowledge, have not been previously considered. We interchange the roles of A and B, and consider the generalized eigenvalue problem $B\mathbf{x} = \lambda^{-1} A\mathbf{x}$. For nonsingular A, the sets

$$(2.3) \qquad\qquad \frac{1}{W(A^{-1}B)}$$

and

$$(2.4) \qquad\qquad \frac{1}{W(BA^{-1})}$$

are also eigenvalue inclusion regions for (1.1). Hereby, division and addition, which is used later in the paper, are interpreted elementwise: for a set S and a number γ we define

$$\frac{1}{S} + \gamma = \left\{ \frac{1}{\zeta} + \gamma : \zeta \in S \right\}.$$

Note that the sets (1.2), (2.1), and (2.2) all reduce to the usual field of values $W(A)$ for the pencil (A, I), where I denotes the identity matrix. The following simple example indicates the potential advantage of the sets (2.1) and (2.2) as inclusion regions, over the set (1.2).

EXAMPLE 2.1. Let $A = \text{diag}(1, 2)$ and $B = \text{diag}(1, -1)$. Note that $0 \in W(B)$. Then the eigenvalues are -2 and 1, and one may verify that the sets (2.1) and (2.2) are equal to the interval $[-2, 1]$, which is the smallest convex spectral inclusion region possible. In contrast to this, the sets (2.3), (2.4), and $W(A, B)$ are all equal to $(-\infty, -2] \cup [1, \infty) \cup \{\infty\}$. For $W(A, B)$ this can be seen from the implication: if $\lambda \in W(A, B)$ then it must hold that $|x_1|^2 + 2|x_2|^2 - \lambda(|x_1|^2 - |x_2|^2) = 0$ together with the constraint $|x_1|^2 + |x_2|^2 = 1$. Here clearly, as inclusion regions, $W(B^{-1}A)$ and $W(AB^{-1})$ are superior to the other three sets.

However, the converse can also hold. In the next example we show a typical case where $W(A, B)$ is a tighter inclusion region than (2.1), (2.2), (2.3), and (2.4): if A is Hermitian, and B is HPD.

EXAMPLE 2.2. We take the matrices A = bcsstk06 and B = bcsstm06 of dimension $n = 420$ from the Matrix Market [6]; this problem arises in structural engineering. A is Hermitian, B is diagonal with positive elements. Since $L^{-1}AL^{-*}$ is Hermitian, $W(A, B) = W(L^{-1}AL^{-*})$ is the ideal convex inclusion region $[\lambda_{\min}, \lambda_{\max}]$; no convex inclusion region can be smaller. The matrices $B^{-1}A$ and AB^{-1} are non-Hermitian, and their field of values is much larger.

As already illustrated by Example 2.1, the sets (2.1), (2.2) on the one hand, and (2.3), (2.4) on the other, differ in nature. $W(B^{-1}A)$ and $W(AB^{-1})$ are closed, bounded, and convex spectral inclusion sets. The set $1/W(A^{-1}B)$ is generally non-convex, and may or may not be unbounded, depending on whether or not $0 \in W(A^{-1}B)$. To be precise, exactly one of the three following cases holds:

- If a neighborhood of the origin is contained in $W(A^{-1}B)$, then (2.3) is unbounded, with bounded complement. This bounded complement may also be considered a spectral *exclusion region*.
- If a neighborhood of the origin is not in $W(A^{-1}B)$, then (2.3) is a bounded inclusion region.
- In the special case that the origin lies on the boundary of $W(A^{-1}B)$, then (2.3) is an unbounded inclusion region with unbounded complement.

Similar remarks hold for the set $1/W(BA^{-1})$. We will study related properties of more general sets in Section 5 (see Proposition 5.4). We provide a further small illustrative example.

EXAMPLE 2.3. Let A and B be 10×10 matrices whose elements are generated randomly with respect to the uniform distribution on $(-\frac{1}{2}, \frac{1}{2})$. In Figure 2.1, we plot the spectrum (dots), together with the sets $W(B^{-1}A)$ (solid), $W(AB^{-1})$ (dash), $1/W(A^{-1}B)$ (dotted line), and $1/W(BA^{-1})$ (dash-dot). The inclusion region $W(AB^{-1})$ is tighter than $W(B^{-1}A)$; the norms $\|AB^{-1}\| \approx 7.9$ and $\|B^{-1}A\| \approx 10.9$ may already serve as indicators of this fact (recall that $W(A)$ is contained in the disk with radius $\|A\|$).

Since a neighborhood of the origin is contained in both $W(A^{-1}B)$ and $W(BA^{-1})$, the sets (2.3) and (2.4) are unbounded inclusion regions, or can also be seen as bounded exclusion regions. Note that a neighborhood of the origin is excluded; we will come back to this phenomenon in Section 5.

We will study generalizations of the sets (2.1), (2.2), (2.3), and (2.4) in Section 5, and show that they are special cases of two more general families of inclusion regions.

3. Approximation of $W(A, B)$ for Hermitian positive definite B. We now consider the numerical approximation of $W(A, B)$ for HPD B; first for small-sized, and subsequently for large-sized pencils. For small-size matrices, $W(A)$ can be efficiently computed by the
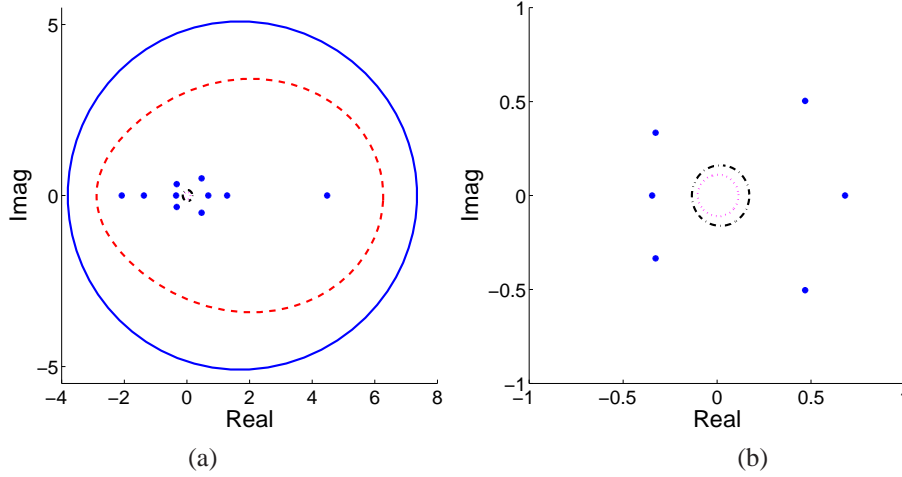
FIG. 2.1. *(a) Eigenvalues (dots), $W(B^{-1}A)$ (solid), $W(AB^{-1})$ (dash), $1/W(A^{-1}B)$ (dot), and $1/W(BA^{-1})$ (dash-dot), for two 10×10 random matrices. The last two sets are better visible in (b), a zoom-in of (a).*

method proposed by Johnson [3]: determine

$$\tfrac{1}{2}\,\lambda_{\max}(e^{i\alpha}A + (e^{i\alpha}A)^*) \quad \text{and} \quad \tfrac{1}{2}\,\lambda_{\min}(e^{i\alpha}A + (e^{i\alpha}A)^*)$$

for a modest number of angles α with $0 \le \alpha < \pi$. Hereby the equalities

$$\max_{\zeta \in W(A)} \text{Re}(\zeta) = \tfrac{1}{2}\,\lambda_{\max}(A + A^*),$$

$$\min_{\zeta \in W(A)} \text{Re}(\zeta) = \tfrac{1}{2}\,\lambda_{\min}(A + A^*)$$

are used for every α. Since for HPD B with decomposition $B = LL^*$ we have $W(A, B) = W(L^{-1}AL^{-*})$, we can also use this approach to efficiently approximate $W(A, B)$ for small and medium sized matrices A and B.

For large sparse HPD matrices B, computing an exact decomposition $B = LL^*$ will often be unattractive. Instead, we can attempt to approximate $W(A, B)$ via projection of A and B onto a low-dimensional subspace $\mathcal{V}$. Let the matrix V have columns that form an orthonormal basis for $\mathcal{V}$. Then we have

$$(3.1) \qquad \left\{ \frac{\mathbf{x}^*A\mathbf{x}}{\mathbf{x}^*B\mathbf{x}} : \mathbf{x} \ne \mathbf{0} \right\} \supseteq \left\{ \frac{\mathbf{c}^*V^*AV\mathbf{c}}{\mathbf{c}^*V^*BV\mathbf{c}} : \mathbf{c} \ne \mathbf{0} \right\}.$$

The expression on the right-hand side may be viewed as the restriction of $W(A, B)$ to the subspace $\mathcal{V}$. Since the projection V^*BV is also HPD, we can decompose $V^*BV = MM^*$, and this set is equal to

$$\left\{ \frac{\mathbf{d}^*M^{-1}V^*AVM^{-*}\mathbf{d}}{\mathbf{d}^*\mathbf{d}} : \mathbf{d} \ne \mathbf{0} \right\} = W(M^{-1}V^*AVM^{-*}).$$

The crucial ingredient is a suitable space $\mathcal{V}$. In view of the transformed eigenvalue problem

$$L^{-1}AL^{-*}\mathbf{y} = \lambda\mathbf{y}, \qquad B = LL^*, \quad \mathbf{y} = L^*\mathbf{x},$$

an ideal candidate would be the Krylov space

$$\mathcal{K}_k(L^{-1}AL^{-*}, \mathbf{v}_1) := \mathrm{span}\{\mathbf{v}_1,\ L^{-1}AL^{-*}\mathbf{v}_1,\ \ldots,\ (L^{-1}AL^{-*})^{k-1}\mathbf{v}_1\}$$

for a certain starting vector $\mathbf{v}_1$ and a modest dimension k, but this is assumed to be computationally expensive. Instead, we can approximate the above Krylov space using an inexact decomposition $B \approx LL^*$, for instance an inexact Cholesky factorization. This gives a new method described in Algorithm 1.

Algorithm 1   A method to approximate $W(A, B)$ for large, HPD B.

Input: A matrix A, a Hermitian positive definite B, starting vector $\mathbf{v}_1$, dimension of Krylov space k, and number of angles m; (inexact) Cholesky factor L of B
Output: An approximation to $W(A, B)$
  1:    Generate a basis V for the Krylov space $\mathcal{K}_k(L^{-1}AL^{-*}, \mathbf{v}_1)$
  2:    Decompose $V^*BV = MM^*$
  3:    Approximate $W(A, B)$ by $W(M^{-1}V^*AVM^{-*})$ using m angles

---

We stress the fact that, whether or not we use the exact Cholesky factor in the generation of the Krylov space, the resulting "inclusion region" is in fact an *approximate* inclusion region due to (3.1). However, although it is therefore not guaranteed that the spectrum is contained in this approximation, this will often be the case in practice. The following experiment indicates the potential of Algorithm 1.

EXPERIMENT 3.1. We take the matrices A = mhd1280a and B = mhd1280b from the Matrix Market [6]; this problem arises in magnetohydrodynamics. B is HPD; its exact Cholesky factor L has 14400 nonzeros. The inexact Cholesky factor L_1 which is generated by the Matlab command L1 = cholinc(B,1e-1) has only about 24% of the nonzeros of L. We carry out Algorithm 1 using L, and using L_1. In Figure 3.1, the spectrum is indicated (dots), together with the inclusion region $W(M^{-1}V^*AVM^{-*})$ based on the Krylov space $\mathcal{K}_{10}(L^{-1}AL^{-*}, \mathbf{v}_1)$ for the exact Cholesky factor L (solid line) and a random starting vector $\mathbf{v}_1$. The dashed line is an approximate inclusion region, obtained in a similar way; the only difference is that the inexact factor L_1 is used. While both inclusion regions are relatively coarse, note that the regions derived with the exact and inexact Cholesky factors are almost indistinguishable. We will return to this example in Section 7.

Note that the use of Algorithm 1 is not limited to the case that B is HPD. If A is HPD, then we can interchange the roles of A and B and in view of

$$W(A, B) = \frac{1}{W(B, A)}$$

we can efficiently approximate the set $W(B, A)$ in this case. Note that, considered as an inclusion region, this set may have drawbacks as mentioned in the previous section: it may be unbounded and non-convex; however, the set can be efficiently computed.

Moreover, if A and B are Hermitian but neither A nor B are positive definite, but a certain linear combination $A + \gamma B$ is HPD, then we may use the following result.

LEMMA 3.2. *For every* $\gamma \in \mathbb{C}$ *we have*

$$W(A, B) = \frac{1}{W(B, A + \gamma B)} - \gamma.$$
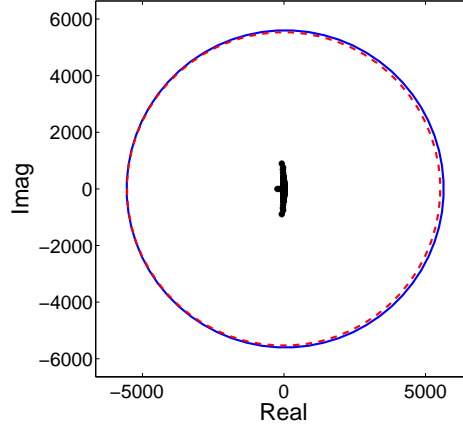
FIG. 3.1. *The spectrum (dots) and (true and approximate) inclusion regions* $W(M^{-1}V^*AVM^{-*})$, *where* V *is a basis for the Krylov space* $\mathcal{K}_{10}(L^{-1}AL^{-*}, \mathbf{v}_1)$, *and* $V^*BV = MM^*$. *While L is the exact Cholesky factor for the solid line, it is an inexact Cholesky factor (drop tolerance 0.1) for the dashed line.*

Proof. If there exists an $\mathbf{x}$ for which $\mathbf{x}^*A\mathbf{x} = \mathbf{x}^*B\mathbf{x} = 0$, both sides are equal to $\mathbb{C} \cup \{\infty\}$. Otherwise we have

$$\frac{1}{W(B, A + \gamma B)} - \gamma = \left\{ \frac{\mathbf{x}^*(A + \gamma B)\,\mathbf{x}}{\mathbf{x}^*B\mathbf{x}} : \mathbf{x} \neq \mathbf{0} \right\} - \gamma$$

$$= \left\{ \frac{\mathbf{x}^*A\mathbf{x}}{\mathbf{x}^*B\mathbf{x}} : \mathbf{x} \neq \mathbf{0} \right\} = W(A, B). \qquad \square$$

In this case we can also apply Algorithm 1. However, it is not obvious how to compute or approximate (1.2) if neither A, nor B, nor any linear combination of A and B is HPD. This is the topic of the next section.

4. Field of values type inclusion regions for non HPD B. Now consider the case in which neither A, nor B, nor any linear combination of A and B is HPD. Psarrakos [7] proposed a method (via the so-called joint numerical range) suitable for pairs (A, B) of which at least one matrix is Hermitian (but not necessary positive definite). This method uses a discretization of the unit sphere $S^2 \subset \mathbb{R}^3$ and for every grid point a maximum eigenvalue of a different associated Hermitian matrix has to be computed. Consequently, this approach does not seem attractive for large pencils. Unlike for Johnson's method (see, e.g., [1]), there does not seem to be a natural approach that generates just one Krylov space for all these eigenvalue problems, since at each grid point a different linear combination of three Hermitian matrices is involved. Of course, one could generate a new Krylov space for each individual grid point, but this drastically increases the amount of work. Moreover, the method in [7] is not suitable for general non-Hermitian pencils.

Therefore, we will further study the spectral inclusion regions $W(B^{-1}A)$, $W(AB^{-1})$, $1/W(A^{-1}B)$, and $1/W(BA^{-1})$ as introduced in Section 2. For small matrices, these sets may be approximated using Johnson's method. We will give an illustration of Psarrakos's approach and some of the mentioned sets in the following simple example, also considered in [7].

EXAMPLE 4.1. Let $A = \begin{bmatrix} 1 & 4 \\ 0 & 3 \end{bmatrix}$ and $B = \begin{bmatrix} 1 & 0 \\ 0 & 0 \end{bmatrix}$ with eigenvalues 1 and ∞. Psarrakos's approach [7] gives an approximation of $W(A, B)$ by taking well-chosen sample vectors $\mathbf{z}$ and computing the corresponding Rayleigh quotients $\frac{\mathbf{z}^*A\mathbf{z}}{\mathbf{z}^*B\mathbf{z}}$; see the dots in Figure 4.1.
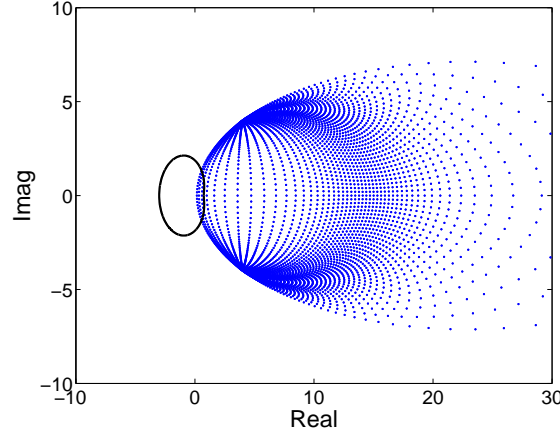
FIG. 4.1. *Psarrakos's approach [7] (dots) and the unbounded inclusion region* $1/W(BA^{-1})$. *The inclusion region* $1/W(A^{-1}B)$ *is the real interval* $[1,\infty)$ *together with the point at infinity.*

The set $1/W(BA^{-1})$ is an unbounded inclusion region, or may also be seen as bounded exclusion region, enclosed by the solid line. This exclusion region is nearly, but not completely, convex. Furthermore, one may verify that $1/W(A^{-1}B)$ is the real interval $[1,\infty)$ together with the point at infinity. Again, $1/W(A^{-1}B)$ as inclusion region is superior to $W(A,B)$. As B is singular, we do not consider (2.1) and (2.2).

For large sparse matrices, the matrix inverses present in the sets $W(B^{-1}A)$, $W(AB^{-1})$, $1/W(A^{-1}B)$, or $1/W(BA^{-1})$ seem problematic for practical use. However, we note that

$$W(B^{-1}A) = \left\{ \frac{\mathbf{x}^*B^{-1}A\mathbf{x}}{\mathbf{x}^*\mathbf{x}} : \mathbf{x} \neq \mathbf{0} \right\} = \left\{ \frac{\mathbf{y}^*AB^*\mathbf{y}}{\mathbf{y}^*BB^*\mathbf{y}} : \mathbf{y} \neq \mathbf{0} \right\} = W(AB^*, BB^*),$$

$$W(AB^{-1}) = \left\{ \frac{\mathbf{x}^*AB^{-1}\mathbf{x}}{\mathbf{x}^*\mathbf{x}} : \mathbf{x} \neq \mathbf{0} \right\} = \left\{ \frac{\mathbf{y}^*B^*A\mathbf{y}}{\mathbf{y}^*B^*B\mathbf{y}} : \mathbf{y} \neq \mathbf{0} \right\} = W(B^*A, B^*B).$$

Moreover,

$$\frac{1}{W(A^{-1}B)} = \left\{ \frac{\mathbf{x}^*\mathbf{x}}{\mathbf{x}^*A^{-1}B\mathbf{x}} : \mathbf{x} \neq \mathbf{0} \right\} = \left\{ \frac{\mathbf{y}^*AA^*\mathbf{y}}{\mathbf{y}^*BA^*\mathbf{y}} : \mathbf{y} \neq \mathbf{0} \right\}$$

$$= W(AA^*, BA^*) = \frac{1}{W(BA^*, AA^*)}$$

$$\frac{1}{W(BA^{-1})} = \left\{ \frac{\mathbf{x}^*\mathbf{x}}{\mathbf{x}^*BA^{-1}\mathbf{x}} : \mathbf{x} \neq \mathbf{0} \right\} = \left\{ \frac{\mathbf{y}^*A^*A\mathbf{y}}{\mathbf{y}^*A^*B\mathbf{y}} : \mathbf{y} \neq \mathbf{0} \right\}$$

$$= W(A^*A, A^*B) = \frac{1}{W(A^*B, A^*A)}.$$

The advantage of the various rightmost expressions is that these sets can be dealt with by the methods of Section 3 since AA^*, A^*A, B^*B, and BB^* are all HPD if A and B are nonsingular.

For large-sized pencils we can therefore use subspace projection methods based on the same idea as behind Algorithm 1; we summarize them in Algorithm 2. For instance, in variant (a), we approximate $W(B^{-1}A) = W(AB^*, B^*B)$ by $W(V^*AB^*V, V^*B^*BV)$, where V contains an orthonormal basis for a Krylov space. Instead of the "exact" Krylov space

$\mathcal{K}_k(B^{-1}A, \mathbf{v}_1)$, we can also use a Krylov space generated with an inexact LU-decomposition of B, that is, use $\mathcal{K}_k(U^{-1}L^{-1}A, \mathbf{v}_1)$, where $B \approx LU$.

We remark that in Steps 2 and 3 of Algorithm 2, some additional computational tricks are used. For instance, for (a), it is not necessary to compute V^*BB^*V and to subsequently determine its Cholesky factor. Instead, we can compute the reduced QR-decomposition $B^*V = QR$. This implies that $V^*BB^*V = R^*R$, so that

$$W(V^*AB^*V, V^*BB^*V) = W(R^{-*}V^*AB^*VR^{-1}) = W(R^{-*}V^*AQ).$$

Similar techniques can be used for (b), (c), and (d): for (b) we have, with $BV = QR$,

$$W(V^*B^*AV, V^*B^*BV) = W(R^{-*}V^*B^*AVR^{-1}) = W(Q^*AVR^{-1}),$$

for (c), with $A^*V = QR$,

$$\frac{1}{W(V^*BA^*V, V^*AA^*V)} = \frac{1}{W(R^{-*}V^*BA^*VR^{-1})} = \frac{1}{W(R^{-*}V^*BQ)},$$

finally, for (d), with $AV = QR$,

$$\frac{1}{W(V^*A^*BV, V^*A^*AV)} = \frac{1}{W(R^{-*}V^*A^*BVR^{-1})} = \frac{1}{W(Q^*BVR^{-1})}.$$

Algorithm 2 Methods to approximate (a) $W(B^{-1}A)$, (b) $W(AB^{-1})$, (c) $1/W(A^{-1}B)$, and/or (d) $1/W(BA^{-1})$ for large B (intended for non HPD B).

Input: Matrices A, B, starting vector $\mathbf{v}_1$, dimension of Krylov space k, and number of angles m; (inexact) LU-factors for A or B.
Output: An approximation to a spectral inclusion region based on a field of values
  1: Approximate the Krylov space
       (a) $\mathcal{K}_k(B^{-1}A, \mathbf{v}_1)$ (b) $\mathcal{K}_k(AB^{-1}, \mathbf{v}_1)$ (c) $\mathcal{K}_k(A^{-1}B, \mathbf{v}_1)$ (d) $\mathcal{K}_k(BA^{-1}, \mathbf{v}_1)$
     by a space $\mathcal{V}$, by working with an (inexact) LU-decomposition
  2: Compute the reduced QR-decomposition
       (a) $B^*V = QR$ (b) $BV = QR$ (c) $A^*V = QR$ (d) $AV = QR$
  3: Approximate the set
       (a) $W(R^{-*}V^*AQ)$ (b) $W(Q^*AVR^{-1})$
       (c) $1/W(R^{-*}V^*BQ)$ (d) $1/W(Q^*BVR^{-1})$
     using Johnson's method with m angles

In the next section, we will study a family of inclusion regions for which the sets (2.1), (2.2), (2.3), and (2.4) are special cases. Finally, we would like to mention that one could also consider approximate inclusion regions of the form $W((V^*BV)^{-1}V^*AV)$. However, these will often not be competitive to the regions generated by Algorithms 1 and 2. If B is HPD, then a symmetric decomposition of V^*BV (as in Algorithm 1) will give superior results, while $W((V^*BV)^{-1}V^*AV)$ is unbounded if $0 \in W(V^*BV)$, which may occur for non-HPD matrices B.

5. Inclusion regions from shifted pencils. In this section, we extend several results from [1] to the context of matrix pencils. Let $\tau \notin \Lambda(A, B)$ which implies that $A - \tau B$ is nonsingular. Because of the shift-and-invert property (cf. (1.1))

$$(5.1) \qquad\qquad (A - \tau B)^{-1}B\mathbf{x} = (\lambda - \tau)^{-1}\mathbf{x},$$

we have for the spectrum $\Lambda(A, B)$ of the pencil (A, B) that

$$\Lambda(A, B) \subset \frac{1}{W((A - \tau B)^{-1} B)} + \tau.$$

Similarly, in view of

$$B(A - \tau B)^{-1} \mathbf{y} = (\lambda - \tau)^{-1} \mathbf{y}, \qquad (A - \tau B)\, \mathbf{x} = \mathbf{y},$$

we have for the spectrum $\Lambda(A, B)$ of the pencil (A, B) that

$$\Lambda(A, B) \subset \frac{1}{W(B(A - \tau B)^{-1})} + \tau.$$

Therefore,

(5.2) $\qquad \dfrac{1}{W((A - \tau B)^{-1} B)} + \tau \qquad \text{and} \qquad \dfrac{1}{W(B(A - \tau B)^{-1})} + \tau,$

parametrized by $\tau \notin \Lambda(A, B)$, are two families of inclusion regions of field of values type. Furthermore, we note that

$$
\begin{aligned}
\frac{1}{W(B(A - \tau B)^{-1})} + \tau &= \left\{ \frac{\mathbf{y}^* \mathbf{y}}{\mathbf{y}^* B(A - \tau B)^{-1} \mathbf{y}} : \mathbf{y} \neq \mathbf{0} \right\} + \tau \\
(5.3) \qquad &= \left\{ \frac{\mathbf{x}^*(A - \tau B)^*(A - \tau B)\,\mathbf{x}}{\mathbf{x}^*(A - \tau B)^* B \mathbf{x}} : \mathbf{x} \neq \mathbf{0} \right\} + \tau \\
&= \left\{ \frac{\mathbf{x}^*(A - \tau B)^* A\,\mathbf{x}}{\mathbf{x}^*(A - \tau B)^* B \mathbf{x}} : \mathbf{x} \neq \mathbf{0} \right\},
\end{aligned}
$$

and

$$
\begin{aligned}
\frac{1}{W((A - \tau B)^{-1} B)} + \tau &= \left\{ \frac{\mathbf{y}^* \mathbf{y}}{\mathbf{y}^*(A - \tau B)^{-1} B \mathbf{y}} : \mathbf{y} \neq \mathbf{0} \right\} + \tau \\
(5.4) \qquad &= \left\{ \frac{\mathbf{x}^*(A - \tau B)(A - \tau B)^* \mathbf{x}}{\mathbf{x}^* B(A - \tau B)^* \mathbf{x}} : \mathbf{x} \neq \mathbf{0} \right\} + \tau \\
&= \left\{ \frac{\mathbf{x}^* A(A - \tau B)^* \mathbf{x}}{\mathbf{x}^* B(A - \tau B)^* \mathbf{x}} : \mathbf{x} \neq \mathbf{0} \right\}.
\end{aligned}
$$

Characterizations (5.3) and (5.4) enable effective computational approaches, since

$$
\frac{1}{W(B(A - \tau B)^{-1})} + \tau = \frac{1}{W((A - \tau B)^* B, \ (A - \tau B)^*(A - \tau B))} + \tau,
$$

$$
\frac{1}{W((A - \tau B)^{-1} B)} + \tau = \frac{1}{W(B(A - \tau B)^*, \ (A - \tau B)(A - \tau B)^*)} + \tau,
$$

where $(A - \tau B)^*(A - \tau B)$ and $(A - \tau B)(A - \tau B)^*$ are HPD.

   For the first family, we consider the subspace approximation

$$
\frac{1}{W(V^*(A - \tau B)^* BV, \ V^*(A - \tau B)^*(A - \tau B)V)} + \tau
$$

where the columns of V are an orthonormal basis for the Krylov space

$$
\mathcal{K}_k(BU^{-1} L^{-1}, \mathbf{v}_1), \qquad A - \tau B \approx LU.
$$

With $(A - \tau B)V = QR$, this yields

$$\frac{1}{W(R^{-*}V^*(A - \tau B)^* BVR^{-1})} + \tau = \frac{1}{W(Q^* BVR^{-1})} + \tau.$$

For the second family, we consider the subspace approximation

$$\frac{1}{W(V^* B(A - \tau B)^* V, \ V^*(A - \tau B)(A - \tau B)^* V)} + \tau$$

where the orthonormal columns of V span the Krylov space $\mathcal{K}_k(U^{-1}L^{-1}B, \mathbf{v}_1)$. Using the QR-decomposition $(A - \tau B)^* V = QR$, we get

$$\frac{1}{W(R^{-*}V^* B(A - \tau B)^* VR^{-1})} + \tau = \frac{1}{W(R^{-*}V^* BQ)} + \tau.$$

These subspace based approximations are summarized in Algorithm 3.

Algorithm 3 Methods to approximate $1/W(B(A - \tau B)^{-1}) + \tau$ or $1/W((A - \tau B)^{-1}B) + \tau$

Input: Matrices A, B, a shift τ, starting vector $\mathbf{v}_1$, dimension of Krylov space k,
    and number of angles m; (inexact) LU-factors for $A - \tau B$.
Output: An approximation to the spectral inclusion regions
        (a) $1/W(B(A - \tau B)^{-1}) + \tau$ or   (b) $1/W((A - \tau B)^{-1}B) + \tau$
  1:    Approximate the Krylov space
        (a) $\mathcal{K}_k(B(A - \tau B)^{-1}, \mathbf{v}_1)$ or   (b) $\mathcal{K}_k((A - \tau B)^{-1}B, \mathbf{v}_1)$
    by a space $\mathcal{V}$, using the (inexact) LU-factors
  2:    Compute the reduced QR-decomposition
        (a) $(A - \tau B)V = QR$ or   (b) $(A - \tau B)^* V = QR$
  3:    Approximate the set
        (a) $1/W(Q^* BVR^{-1}) + \tau$ or   (b) $1/W(R^{-*}V^* BQ) + \tau$
    using Johnson's method with m angles

We note that a disadvantage of this approach is that in principle we need a different Krylov subspace for every τ. In the remainder of this section we study several properties of the two families (5.2). The next results can be viewed as extensions of [1, Thm. 5].

LEMMA 5.1.

$$(a) \quad \lim_{|\tau| \to \infty} \frac{1}{W(B(A - \tau B)^{-1})} + \tau = W(B^*A, B^*B),$$

$$(b) \quad \lim_{\tau \to 0} \frac{1}{W(B(A - \tau B)^{-1})} + \tau = W(A^*A, A^*B),$$

$$(c) \quad \lim_{|\tau| \to \infty} \frac{1}{W((A - \tau B)^{-1}B)} + \tau = W(AB^*, BB^*),$$

$$(d) \quad \lim_{\tau \to 0} \frac{1}{W((A - \tau B)^{-1}B)} + \tau = W(AA^*, BA^*).$$

Proof. For $\tau \neq 0$ there holds (cf. also (5.3))

$$\frac{1}{W(B(A - \tau B)^{-1})} + \tau = \left\{ \frac{\mathbf{x}^*(A - \tau B)^* A\mathbf{x}}{\mathbf{x}^*(A - \tau B)^* B\mathbf{x}} : \mathbf{x} \neq \mathbf{0} \right\} = \left\{ \frac{\mathbf{x}^*(\frac{1}{\tau}A - B)^* A\mathbf{x}}{\mathbf{x}^*(\frac{1}{\tau}A - B)^* B\mathbf{x}} : \mathbf{x} \neq \mathbf{0} \right\}$$

from which (a) and (b) follow. Parts (c) and (d) are proved similarly.   □

Some remarks about these results are in order. If A and B are nonsingular, then the sets in this lemma are $W(AB^{-1})$, $1/W(BA^{-1})$, $W(B^{-1}A)$, and $1/W(A^{-1}B)$ respectively. From these properties we see that the sets (2.1), (2.2), (2.3), and (2.4) studied in Section 4 are in fact special cases of the families (5.2). Moreover, the limit sets in (a) and (c) are the only members of these two families that are guaranteed to be convex.

Next, we present extensions of [1, Thms. 2 and 4] for matrix pencils.

THEOREM 5.2. *Let G be a set-valued function from the set of $n \times n$ matrices to subsets of $\mathbb{C}$, such that for any A the set $G(A)$ is bounded and contains $\Lambda(A)$. Then*

$$\Lambda(A, B) = \bigcap_{\tau \in \mathbb{C} \setminus \Lambda(A,B)} \frac{1}{G((A - \tau B)^{-1} B)} + \tau,$$

$$\Lambda(A, B) = \bigcap_{\tau \in \mathbb{C} \setminus \Lambda(A,B)} \frac{1}{G(B(A - \tau B)^{-1})} + \tau.$$

Proof. Since $\Lambda(A, B) \subset \frac{1}{G((A-\tau B)^{-1}B)} + \tau$ for all $\tau \notin \Lambda(A, B)$, we have that $\Lambda(A, B)$ is also contained in the intersection. To show that equality holds, suppose that $\zeta \notin \Lambda(A, B)$, then $\zeta \notin \frac{1}{G((A-\zeta B)^{-1}B)} + \zeta$, since $G((A - \zeta B)^{-1}B)$ is a bounded set. The second statement is proved similarly. $\quad\square$

Since the field of values satisfies the requirements of Theorem 5.2, we immediately get the following result.

COROLLARY 5.3. *We have the intersection properties*

$$\Lambda(A, B) = \bigcap_{\tau \in \mathbb{C} \setminus \Lambda(A,B)} \frac{1}{W((A - \tau B)^{-1} B)} + \tau,$$

$$\Lambda(A, B) = \bigcap_{\tau \in \mathbb{C} \setminus \Lambda(A,B)} \frac{1}{W(B(A - \tau B)^{-1})} + \tau.$$

If $0 \notin W((A - \tau B)^{-1} B)$, then the set $1/W((A - \tau B)^{-1} B) + \tau$ is bounded and hence may be seen as an inclusion region. If $0 \in W((A - \tau B)^{-1} B)$, then $1/W((A - \tau B)^{-1} B) + \tau$ is unbounded. If its complement is bounded, it may be more convenient to view this complement as an *exclusion region*. We will call the case in which both the inclusion region $1/W((A - \tau B)^{-1} B) + \tau$ and its complement are unbounded the *transition case*.

The next proposition, an extension of [1, Thm. 6], implies that the transition case for $1/W((A - \tau B)^{-1} B) + \tau$ occurs precisely if $\tau \in \partial W(B^{-1}A)$ (that is, on the boundary of $W(B^{-1}A)$) and, similarly, that the transition case for $1/W(B(A - \tau B)^{-1}) + \tau$ occurs precisely if $\tau \in \partial W(AB^{-1})$.

PROPOSITION 5.4. *Let $\tau \notin \Lambda(A, B)$ and B be nonsingular. Then*
(a) $0 \in W((A - \tau B)^{-1} B)$ if and only if $\tau \in W(B^{-1}A)$,
(b) $0 \in W(B(A - \tau B)^{-1})$ if and only if $\tau \in W(AB^{-1})$.
Proof. Since

$$W((A - \tau B)^{-1} B) = \left\{ \frac{\mathbf{x}^* B(A - \tau B)^* \mathbf{x}}{\mathbf{x}^* (A - \tau B)(A - \tau B)^* \mathbf{x}} : \mathbf{x} \neq \mathbf{0} \right\},$$

$0 \in W((A - \tau B)^{-1} B)$ if and only if there exists a nonzero $\mathbf{x}$ such that $\mathbf{x}^* B(A - \tau B)^* \mathbf{x} = 0$ which means that $\tau \in W(AB^*, BB^*)$, and since B is nonsingular this is equal to the set $W(B^{-1}A)$. The proof of the second statement is similar. $\quad\square$

The following result, an extension of [1, Prop. 3], indicates that by considering (5.2), we can get inclusion regions *excluding* (user-chosen) targets τ.

PROPOSITION 5.5.

$$\text{dist}\left(\tau, \ \frac{1}{W((A - \tau B)^{-1}B)} + \tau\right) \geq \|(A - \tau B)^{-1}B\|^{-1},$$

$$\text{dist}\left(\tau, \ \frac{1}{W(B(A - \tau B)^{-1})} + \tau\right) \geq \|B(A - \tau B)^{-1}\|^{-1}.$$

Proof. The first statement follows directly from the facts that the set $W((A - \tau B)^{-1}B)$ is contained in the disk around the origin with radius $\|(A - \tau B)^{-1}B\|$. The second statement follows from a similar argument. ☐

In fact, we have already seen examples of this in Figures 2.1 and 3.1. We will make fruitful use of this fact in Section 7.

6. Relation with harmonic Rayleigh–Ritz methods. In this section we will first briefly review the harmonic Rayleigh–Ritz method for the generalized eigenvalue problem (see also [8]), and then point out connections with the families of inclusion regions of the previous section.

In subspace methods for eigenvalue problems, one attempts to find approximate eigenpairs $(\theta, \mathbf{v}) \approx (\lambda, \mathbf{x})$ of which the approximate eigenvector $\mathbf{v}$ is sought in a low-dimensional search space $\mathcal{V}$. The standard Ritz–Galerkin projection

$$A\mathbf{v} - \theta B\mathbf{v} \perp \mathcal{V}$$

is frequently employed to find eigenvalues at the exterior of the spectrum, but is often less successful to approximate interior eigenvalues.

Suppose we are interested in eigenpairs close to a target $\tau \in \mathbb{C}\backslash\Lambda(A, B)$. Because of the shift-and-invert property (5.1), interior eigenvalues close to τ are exterior eigenvalues of $(A - \tau B)^{-1}B$. This suggests to impose the Galerkin condition

$$(A - \tau B)^{-1}B\mathbf{v} - (\theta - \tau)^{-1}\mathbf{v} \perp \mathcal{W}$$

for a certain test space $\mathcal{W}$. With the choice $\mathcal{W} = (A - \tau B)^*(A - \tau B)\mathcal{V}$ we manage to avoid matrix inverses and get the harmonic Ritz extraction

$$V^*(A - \tau B)^*(A - \tau B)V\mathbf{c} = (\theta - \tau)V^*(A - \tau B)^*BV\mathbf{c},$$

where $\mathbf{v} = V\mathbf{c}$ are the harmonic Ritz vectors. The corresponding harmonic Ritz values are given by

$$\theta = \frac{\mathbf{c}^*V^*(A - \tau B)^*(A - \tau B)V\mathbf{c}}{\mathbf{c}^*V^*(A - \tau B)^*BV\mathbf{c}} + \tau = \frac{\mathbf{c}^*V^*(A - \tau B)^*AV\mathbf{c}}{\mathbf{c}^*V^*(A - \tau B)^*BV\mathbf{c}}.$$

Therefore, we conclude that for fixed τ, (5.3) is exactly the set of all possible harmonic Ritz values that can be obtained from a one-dimensional subspace $\mathcal{V}$.

To obtain the set (5.4), we now consider the following new *left-harmonic Ritz approach*. We start with the shift-and-invert property

$$(A - \tau B)^{-*}B^*\mathbf{y} = (\lambda - \tau)^{-*}\mathbf{y}.$$

(In this case, $\mathbf{y}$ represents a left eigenvector; but since we are interested in the eigenvalues in this context, this is irrelevant.) This inspires us to extract an approximate eigenpair $(\theta, \mathbf{v})$ by the Galerkin condition

$$(A - \tau B)^{-*}B^*\mathbf{v} - (\theta - \tau)^{-*}\mathbf{v} \perp \mathcal{W},$$

for a certain test space $\mathcal{W}$. With $\mathcal{W} = (A - \tau B)(A - \tau B)^*\mathcal{V}$ we get the harmonic Ritz extraction

$$V^*(A - \tau B)(A - \tau B)^*\mathbf{v} = (\theta - \tau)^*V^*(A - \tau B)B^*\mathbf{v}.$$

where we call the vectors $\mathbf{v} = V\mathbf{c}$ the left-harmonic Ritz vectors. The corresponding left-harmonic Ritz values are given by

$$\theta = \frac{\mathbf{c}^*V^*(A - \tau B)(A - \tau B)^*V\mathbf{c}}{\mathbf{c}^*V^*B(A - \tau B)^*V\mathbf{c}} + \tau = \frac{\mathbf{c}^*V^*A(A - \tau B)^*V\mathbf{c}}{\mathbf{c}^*V^*B(A - \tau B)^*V\mathbf{c}}.$$

Hence, we may conclude that for fixed τ, (5.4) is exactly the set of all possible left-harmonic Ritz values that can be obtained from a one-dimensional subspace $\mathcal{V}$.

7. An automated algorithm and a numerical experiment. Algorithm 3 raises the important question how to choose relevant targets τ. Although the user is free to choose any $\tau \notin \Lambda(A, B)$, it is attractive to develop an algorithm that automatically chooses sensible values for τ. Recall from Section 5 that for a chosen τ, Algorithm 3 generates an approximate inclusion region that *excludes* a neighborhood of this τ.

Algorithm 1 (for HPD B) and Algorithm 2 parts (a) and (b) (for non HPD B) provide us with bounded convex (approximate) inclusion regions. These regions may be not very strict; cf. Figures 2.1 and 3.1. If we would like to improve this inclusion region, it seems a promising idea to take the discretized boundary points of the obtained inclusion region as our points for τ, as this "cuts away" parts of our initial inclusion region (cf. also [1]). This leads to an automated "master" Algorithm 4, that calls Algorithms 1, 2, and 3 as appropriate.

Algorithm 4   An automated method to generate an approximate inclusion region

Input: Matrices A, B, starting vector $\mathbf{v}_1$, dimension of Krylov space k, drop tolerance δ,
         and number of angles m.
Output: An approximated spectral inclusion region, consisting of the intersection of
         $\mathcal{O}(m)$ inclusion regions
     if B is HPD
1:       Determine an inexact Cholesky factor of B with drop tolerance δ
2:       Carry out Algorithm 1
     else
3:       Determine inexact LU-factors of B with drop tolerance δ
4:       Carry out Algorithm 2, parts (a) and/or (b)
     end
     for each τ_j on the discretized boundary found in Step 2 or 4
5:       Determine inexact LU-factors of $A - \tau_j B$ with drop tolerance δ
6:       Carry out Algorithm 3, parts (a) and/or (b)
     end

To test Algorithm 4, we return to the setting of Experiment 3.1. Since B is HPD, Algorithm 4 first calls Algorithm 1, which approximates $W(A, B)$. There are two different approximating aspects involved: we project $W(A, B)$ onto a 10-dimensional Krylov space

($k = 10$), and to generate the Krylov space we use an inexact Cholesky decomposition ($\delta = 10^{-5}$, with random $\mathbf{v}_1$). The resulting approximation is a convex inclusion region. For clarity we discretize this region using just 8 points (corner points in Figure 7.1(a)).

Apparently, this is a quite coarse inclusion region; to make it tighter we take the 8 corner points as τ-values. The blue dashed lines indicate approximations to $1/W(B(A-\tau B)^{-1})+\tau$ as described in Algorithm 3(a). These represent finite approximate inclusion regions; note that these regions are not true inclusion regions in this example. The black dotted lines indicate approximations to $1/W((A-\tau B)^{-1}B) + \tau$ as given in Algorithm 3(b). These 8 sets are unbounded inclusion regions. We see that the approximate inclusion region consisting of the intersection of all approximate inclusion regions indeed includes the vast majority of the eigenvalues. Although it does not include some relative outliers, it gives a very good indication of the location of the spectrum.
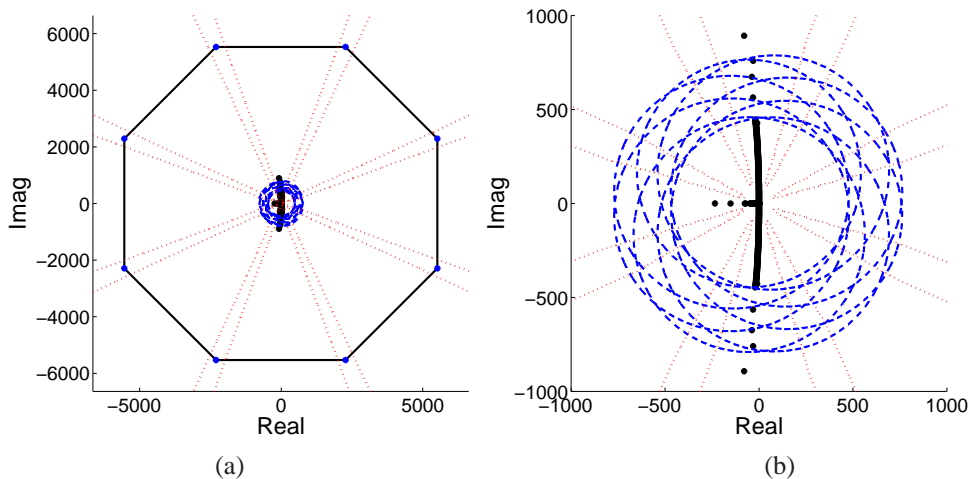
FIG. 7.1. *(a) Result of running Algorithm 4 on the problem from magnetohydrodynamics for the discretization of $W(A, B)$ using 8 points. The blue dashed lines represent inclusion regions obtained with Algorithm 3(a), the black dotted lines those obtained with Algorithm 3(b). Both take for τ the values on the discretized boundary of the approximation of $W(A, B)$ (the 8 corner points). (b) Zoom-in of (a).*

8. Conclusions. Our focus in this paper was on inclusion regions for matrix pencils based on fields of values. We stress that the computation of inclusion regions may be an efficient technique: since the field of values is often well approximated from a low-dimensional Krylov space, *computing a spectral inclusion region may be cheaper than computing even one single eigenvalue!*

Several results in this paper are extensions of results in [1], but for matrix pencils there are many new aspects as well. First, we have slightly modified the usual definition of $W(A, B)$ by adding ∞ if B is singular. We have given procedures to numerically approximate $W(A, B)$ for HPD matrices B (or any combination of A and B), for both matrices of small and large (see Algorithm 1) dimension.

Psarrakos's method [7] can be used for pairs of small dimension of which at least one of the two matrices is Hermitian (and not necessary definite), but seems to be computationally unattractive for large matrices A and B. Moreover, it is not clear from [7] how to effectively approximate $W(A, B)$ if both matrices are non-Hermitian. Apart from this, we have seen that $W(A, B)$ as inclusion region may not reveal much useful information, since it may be very large or even unbounded.

The sets $W(B^{-1}A)$, $W(AB^{-1})$, $1/W(B^{-1}A)$, and $1/W(AB^{-1})$ may be more informative inclusion regions, although the latter two sets may also be unbounded. Of course, the intersection of these sets is also a bounded inclusion region. In contrast to $W(A, B)$, these sets can efficiently be approximated if no linear combination of A and B is HPD (Algorithm 2).

We introduced two families of inclusion regions involving shifted and inverted pencils: $1/W(B(A - \tau B)^{-1}) + \tau$ and $1/W((A - \tau B)^{-1}B) + \tau$, of which the four sets mentioned above are special cases. We considered several theoretical properties as well as their use in practical contexts (Algorithm 3). By varying the shift, we may generate as many inclusion (or exclusion) regions as we desire, depending on the region of the complex plane that is of interest to us.

We pointed out connections with the usual harmonic Rayleigh–Ritz method, as well as a new left-harmonic variant. Finally, we proposed a method that automatically selects targets τ, and gives a bounded approximated inclusion region consisting of the intersection of a user-chosen number of inclusion regions (Algorithm 4).

Acknowledgment. The author thanks the referee for useful and encouraging comments.

REFERENCES

[1] M. E. HOCHSTENBACH, D. A. SINGER, AND P. F. ZACHLIN, *Eigenvalue inclusion regions from inverses of shifted matrices*, Linear Algebra Appl., 429 (2008), pp. 2481–2496.
[2] R. A. HORN AND C. R. JOHNSON, *Topics in Matrix Analysis*, Cambridge University Press, Cambridge, 1991.
[3] C. R. JOHNSON, *Numerical determination of the field of values of a general complex matrix*, SIAM J. Numer. Anal., 15 (1978), pp. 595–602.
[4] C.-K. LI AND L. RODMAN, *Numerical range of matrix polynomials*, SIAM J. Matrix Anal. Appl., 15 (1994), pp. 1256–1265.
[5] D. LOGHIN, M. VAN GIJZEN, AND E. JONKERS, *Bounds on the eigenvalue range and on the field of values of non-Hermitian and indefinite finite element matrices*, J. Comput. Appl. Math., 189 (2006), pp. 304–323.
[6] *The Matrix Market*, a repository for test matrices. http://math.nist.gov/MatrixMarket
[7] P. J. PSARRAKOS, *Numerical range of linear pencils*, Linear Algebra Appl., 317 (2000), pp. 127–141.
[8] G. W. STEWART, *Matrix Algorithms. Vol. II*, SIAM, Philadelphia, 2001.